ELSEVIER

Journal of Alloys and Compounds 446–447 (2007) 124–128

Journal of ALLOYS AND COMPOUNDS

www.elsevier.com/locate/jallcom

Mg_3Mm compound based hydrogen storage materials

L.Z. Ouyang, H.W. Dong, M. Zhu *

School of Mechanical Engineering, South China University of Technology, Guangzhou 510641, People's Republic of China

Received 20 September 2006; received in revised form 28 February 2007; accepted 28 February 2007
Available online 12 March 2007

Abstract

Hydrogen storage properties, composition and phase structures of the Mg–Mm (Mm is abbreviated for misch metal) and Mg–Mm–Ni alloys prepared by induction melting were investigated by X-ray diffraction (XRD), energy dispersive X-ray spectroscopy (EDX) and pressure–composition-isotherms (PCIs) measurement. It has been found that the Mg_3Mm compound with the $D0_3$ structure can absorb hydrogen at room temperature with rapid hydriding kinetics. The desorption of hydrogen of Mg_3Mm and $Mg_3MmNi_{0.1}$ alloys takes place at 281 and 250 °C and the reversible hydrogen storage capacities reach 2.91 and 2.51 wt.%, respectively. The enthalpy (ΔH) and entropy (ΔS) of Mg_3Mm–H dehydriding reaction were determined by using van't Hoff plot. Hydrogen absorption kinetics of the Mg_3Mm alloy at room temperature was also measured and the experimental curves can be well fitted by using Avrami–Erofeev equation.
© 2007 Elsevier B.V. All rights reserved.

Keywords: Metal hydrides; Rare-earth alloys and compounds; Thermodynamic; X-ray diffraction

1. Introduction

Hydrogen may play a key role in the future clean and renewable energy system. Among the major hydrogen storage alloys developed so far, Mg based alloys have been considered as candidates with significant potential owing to their high hydrogen storage capacity (up to 7.6 wt.% in the form of MgH_2), low cost and abundant resource. However, the kinetic properties, hydrogen absorption/desorption temperature and pressure of dehydriding in those materials are not suitable for practical application yet. In order to improve the kinetic properties of Mg based alloys, different methods, such as alloying element substitution [1–3], catalysts addition [4,5], surface modification [6] and non-equilibrium microstructure formation [7–9] have been applied. Although many new results have been reported, the kinetics properties for those materials are still a key problem to be solved.

It is also well known that the intermetallic compounds for hydrogen storage are generally composed of hydrogen-absorb elements (A) and none hydrogen-absorb elements (B) except for Mg–rare-earth metal (Mg-RE) systems [10], such as La_2Mg_{17}, $CeMg_{12}$, Ce_5Mg_{41} and so on. Both RE and Mg could react with H and form hydrides with large negative enthalpy of formation. However, for the alloys in Mg–RE systems, the hydrogen absorption/desorption temperature is too high to be applied although the hydrogen storage content of those compounds is high. For instance, La_2Mg_{17}, with storage content being about 6 wt.%, absorbs hydrogen at about 350 °C [11]. Furthermore, another fatal drawback of Mg–RE compound is its disproportionating reaction, i.e., La_2Mg_{17} transformed to LaH_3 and MgH_2, in hydriding process, which leads to a serious degradation in the hydrogen absorption/desorption process. Early in 1976 [12], Mg_3RE type compounds had been reported to has a structure of $D0_3$ type (space group $Fm3m$), and later in 1984 [13], the possibility of hydrogen storage in Mg_3RE type compound was considered. Very recently, Kamegawa et al. [14] synthesized Mg_3REH_9 phase, of which the crystal structure has not been identified yet, under very high pressure (5 GPa). The theoretical hydrogen storage capacity of Mg_3LaH_9 phase is 4.1 wt.%. Zhang et al. [15] also reported the phase transformation of Mg_3La during the hydrogenation process and Ouyang et al. [16] reported the hydrogen storage property of Mg_3La compound. It has been demonstrated [16] that the reversible hydrogen storage content of Mg_3La compound is 2.89 wt.% under moderate pressure. Mg_3La compound could absorb hydrogen at room temperature and desorb hydrogen at 274 °C.

* Corresponding author.
E-mail address: memzhu@scut.edu.cn (M. Zhu).

0925-8388/$ – see front matter © 2007 Elsevier B.V. All rights reserved.
doi:10.1016/j.jallcom.2007.02.160

Considering the cost of the pure rare-earth metals and commercial application, it is significant to replace pure rare-earth metal by misch metal. The present paper reports the hydrogen storage property of Mg_3Mm based alloys and the effect caused by adding alloying element Ni. It has been found that the intermetallic compound Mg_3Mm can be hydrided under 1 atm H_2 pressure. The maximum reversible hydrogen storage content reaches 2.91 wt.%. In order to obtain some fundamental knowledge and to understand the hydrogen storage behavior of Mg_3RE based alloys, the hydrogen absorption/desorption kinetics and the thermodynamic parameters of these alloys, such as entropy (ΔS) and enthalpy (ΔH) of the reaction, have been studied. The effect of Ni addition on the hydrogen storage properties of this alloy has also been investigated. The preliminary results obtained in this work demonstrate that Mg_3Mm based alloys are promising candidate materials for hydrogen storage.

2. Experimental

Mg_3Mm and $Mg_3MmNi_{0.1}$ alloy ingots were prepared by induction melting of high purity Mg (99.9%), Mm (56.0 at% La, 31.0 at% Nd, 5.0 at% Ce, 8.0 at% Pr) and Ni (99.9%) in a alumina crucible under protection of pure Ar atmosphere with a purity of 99.999%. The alloys were pulverized by ball milling under an argon atmosphere. The phase structures of the Mg_3Mm and $Mg_3MmNi_{0.1}$ alloys were characterized by a Philips X'Pert MPD X-ray diffractometer with Cu Kα radiation. The chemical composition of the alloys was examined by an EDX accessory attached to a Philips XL-30 FEG scanning electron microscope (SEM).

The hydrogen absorption and desorption properties of Mg_3Mm and $Mg_3MmNi_{0.1}$ alloys were measured by PCIs using an Advanced Materials Corporation (AMC) gas reaction controller. The measurement conditions were set as: delay time 30 s, maximum pressure 4.8 MPa. The data of pressure plateau was taken as the middle point of plateau region since the plateau region is not fully flat. The total weight of the sample subjected to PCIs measurements is 1.623 and 1.204 g for Mg_3Mm and $Mg_3MmNi_{0.1}$ alloys, respectively.

3. Results and discussion

3.1. Structure of Mg_3Mm and $Mg_3MmNi_{0.1}$ alloys

Fig. 1(a) and (b) are XRD patterns of the as melted Mg_3Mm and $Mg_3MmNi_{0.1}$ alloys, respectively. As shown in Fig. 1(a), there are 16 diffraction peaks which can be excellently indexed with $D0_3$ structure (BiF_3 type, space group $Fm3m$). The lattice constant of this phase (denoted as Mg_3RE here and below) is 0.7451 nm, which was determined by XRD analysis using Cohen's extrapolation method. The obtained lattice constant of Mg_3RE is a little smaller than that of Mg_3La reported (0.7467 nm, with no detailed composition) by Buschow [12]. Till now, there is no detail data of composition range of Mg_3RE phase in the phase diagram of Mg–Mm system. Here in this work, as determined by EDX analysis, the composition of the actual Mg_3Mm alloy is 72.28 at% Mg, 14.90 at% La, 0.83 at% Ce, 4.02 at% Pr and 7.97 at% Nd. The amount of Mg is a little lower than the nominal composition, 75 at% Mg, of the Mg_3RE compound, which is due to the weight loss during induction melting. However, no other phase was observed in the sample, although there is deficiency in Mg content from stoichiometry, which means that the composition of Mg_3RE phase can be extended to a certain composition range from the stoichiometry of Mg_3RE.

With respect to $Mg_3MmNi_{0.1}$ alloy, as shown in Fig. 1(b), besides the 16 peaks from Mg_3RE phase, there are other diffraction peaks. These peaks can be indexed as a C-centered orthorhombic $MgAl_2Cu$-type structured phase. The morphology of the $Mg_3MmNi_{0.1}$ alloy is shown in Fig. 2. Judging from Fig. 2, $Mg_3MmNi_{0.1}$ alloy is composed of two phases. As determined by EDX analysis, the composition of the secondary phase is 55.59 at% Mg, 16.75 at% Ni, 17.96 at% La, 1.17 at% Ce, 3.06 at% Pr and 5.48 at% Nd, which can be formulated as $Mg_2MmNi_{0.7}$. According to the structure and composition analysis, the secondary phase was determined to be Mg_2MmNi phase (denoted as Mg_2RENi here and below), but a little deviated from stoichiometry ration of Mg_2RENi. The lattice constant of Mg_2RENi phase (a: 4.21, b: 10.27, c: 8.34), as determined from XRD analysis, in this alloy is in agreement with that reported before [16,17]. On the other hand, the composition of the Mg_3RE matrix phase in the alloy is 72.23 at% Mg, 13.53 at% La, 0.0 at% Ce, 4.02 at% Pr and 10.22 at% Nd. The above results reveal that the $Mg_3MmNi_{0.1}$ alloy is composed of Mg_3RE ($D0_3$ structure) and Mg_2RENi ($MgAl_2Cu$-type structure phases). Judging from the composition in the Mg_3RE phase determined by EDX anal-

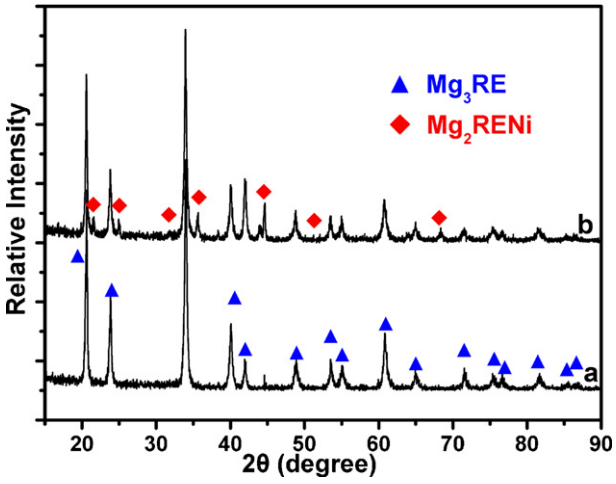

Fig. 1. XRD patterns of the as melted Mg_3Mm (a) and $Mg_3MmNi_{0.1}$ (b) alloys.

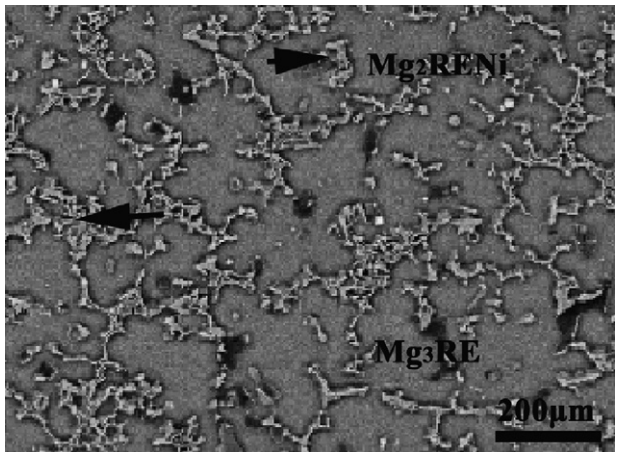

Fig. 2. The morphology of the $Mg_3MmNi_{0.1}$ alloy.

ysis, little Ni dissolved into the Mg_3RE phase in $Mg_3MmNi_{0.1}$ alloy. The lattice constant of Mg_3RE phases in $Mg_3MmNi_{0.1}$ alloy is 0.7451 nm, which is the same as that in Mg_3Mm alloy, is also an evident that little Ni dissolve in the matrix phase.

3.2. Structures of hydrogenated Mg_3Mm and $Mg_3MmNi_{0.1}$ alloys

Fig. 3(a) and (b) are XRD patterns of the hydrogenated Mg_3Mm and $Mg_3MmNi_{0.1}$ alloys, respectively. For Mg_3Mm alloy, as shown in Fig. 3(a), all the diffraction peaks from $D0_3$ structured Mg_3RE disappeared and the newly appeared diffraction peaks from the hydride can be excellently indexed as an fcc lattice. The lattice constant of the fcc structured hydride phase is 0.5605(6) nm as determined by XRD analysis. It means that a structure transition happened during the hydrogenation process. However, the details of the crystal structure, position of hydrogen atoms of this hydride and the mechanism of structure transition require further investigation. It should be noted that a small amount of MgH_2 phase appeared in addition to the major hydride phase. The appearance of MgH_2 phase is probably due to partial disproportionation of Mg_3RE phase in hydriding process. For the hydrogenated $Mg_3MmNi_{0.1}$ alloy, as it is shown in Fig. 3(b), the diffraction peaks of both Mg_3RE and Mg_2RENi disappeared and the newly appeared diffraction peaks from hydride phase can also be excellently indexed as an fcc structure. The fcc structured phase should be transformed from Mg_3RE phase in hydrogenation process as described before. The disappearing of Mg_2RENi phase is also probably due to transformation of this phase to hydride in the hydrogenation process. It has been reported that the Mg_2RENi react with hydrogen to yield a quaternary metal hydride of composition Mg_2RENiH_7 as reported by Renaudin et al. [17]. In the hydrogenated sample of the present work, diffraction peaks other than the unknown fcc structured phase were observed as shown in Fig. 3(b). The peak position is in accordance with that of Mg_2RENiH_7. However, the peaks are too broad and the back ground intensity of the diffractogram is rather strong. A precise analysis of those peaks requires further study. In addition, two plateaus were observed in PCIs curves as shown in Fig. 4(b), which will be illustrated later. These results strongly suggested that both the Mg_3RE and Mg_2RENi phases react with hydrogen during the hydrogenation/dehydrogenation process in $Mg_3MmNi_{0.1}$ alloy. In order to clarify the structure transition process of the Mg_3Mm and $Mg_3MmNi_{0.1}$ alloy, more work is required to reveal the mechanism of the appearance of MgH_2 and transition of Mg_3RE to fcc phase in hydrogenation process.

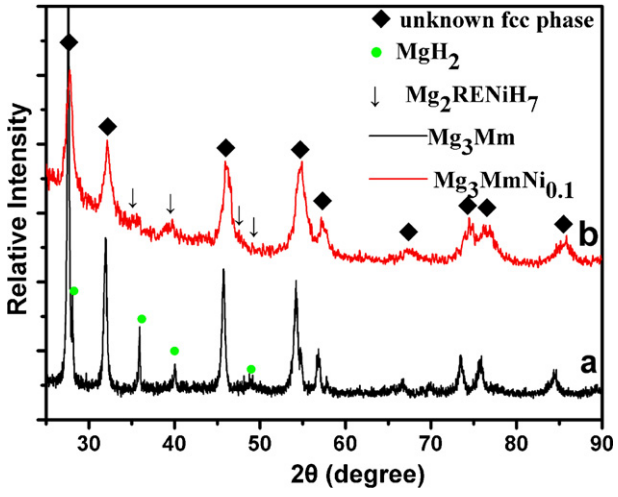

Fig. 3. XRD patterns of the as hydrogenated Mg_3Mm (a) and $Mg_3MmNi_{0.1}$ (b) alloys. The peaks of the unknown can be well indexed by fcc structure.

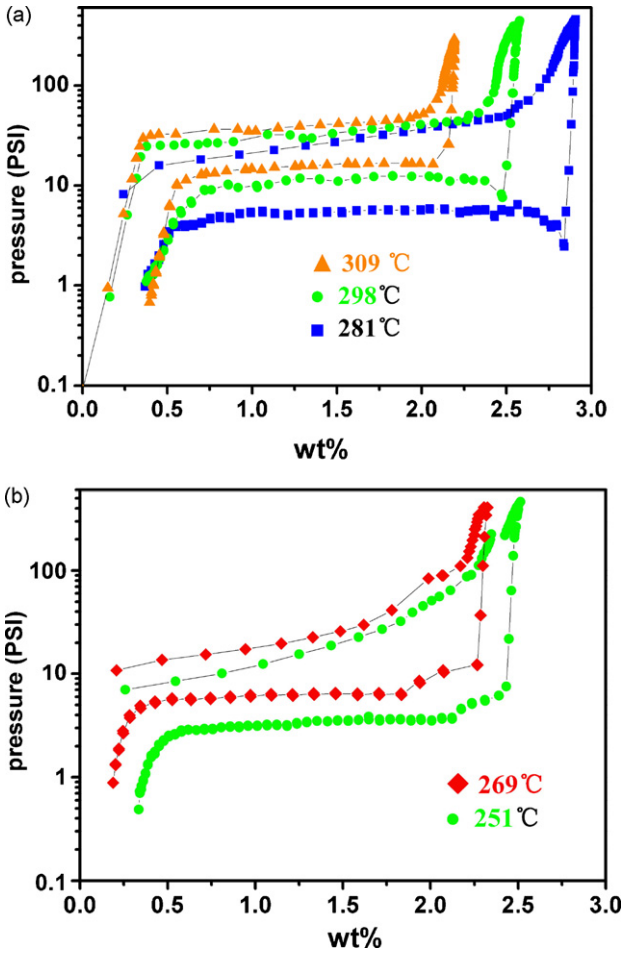

Fig. 4. PCI curves of Mg_3Mm alloys (a) and $Mg_3MmNi_{0.1}$ alloy (b) measured at different temperature.

3.3. Hydrogen storage properties of Mg_3Mm and $Mg_3MmNi_{0.1}$ alloy

Hydrogen storage properties of the Mg_3Mm and $Mg_3MmNi_{0.1}$ alloys were determined by measuring PCIs at different temperature and the results were given in Fig. 4(a) and (b). As it is demonstrated by the PCI measurement, the maximum hydrogen absorption content of Mg_3Mm and $Mg_3Mm_{0.9}Ni_{0.1}$ alloys are 2.91 and 2.51 wt.%, which were measured at 281 and 251 °C, respectively. It is noted that the slope of the plateau of PCIs curves are quite flat. In fact, the Mg_3Mm and $Mg_3MmNi_{0.1}$ alloys can absorb hydrogen

at room temperature after activated by only one hydrogenation/dehydrogenation cycle. It took only several minutes to uptake hydrogen to 90% of its full hydrogen storage content at room temperature. However, the desorption of hydrogen occurs at relatively high temperature. The lowest temperature for hydrogen desorption is 281 and 251 °C for Mg_3Mm and $Mg_3MmNi_{0.1}$ alloys, respectively. Obviously, the addition of Ni lowers the hydrogen desorption temperature, but the hydrogen absorption capacity of $Mg_3MmNi_{0.1}$ alloys also decreases a little. This is towing to the formation of Mg_2RENi phase, of which the theoretical capacity is only 2.8 wt.%, in $Mg_3MmNi_{0.1}$ alloy. It is noted that there are two plateaus in the PCI curves of $Mg_3MmNi_{0.1}$ alloy, as shown in Fig. 4(b). According to this PCI result, there should be two phases undergone hydrogenation/dehydrogenation process. Since Mg_3RE is the major phase, the narrow plateau at high pressure should correspond to the hydriding/dehydriding of Mg_2RENi phase, while the wide plateau at low pressure should correspond to the hydriding/dehydriding of Mg_3RE phase. The PCIs curves of Mg_3Mm and $Mg_3MmNi_{0.1}$ alloys almost remained unchanged after 15 hydrogenation/dehydrogenation cycles carried out by measuring the PCIs curves. This preliminary result reveals that the hydrogen storage properties of Mg_3Mm based alloy are stable in hydrogenation and dehydrogenation cycles. It should be pointed that the accidents fall in pressure occurring at the beginning of the desorption of Mg_3Mm alloy was due to the sluggish dehydrogenation at relative low temperature at the beginning of dehydrogenation process, saying 281 and 298 °C as shown in Fig. 4(a), while at the relative high temperature, saying 309 °C, there is no fall.

According to the PCIs curve of Mg_3Mm alloys measured at different temperatures, ΔH and ΔS for the dehydriding reaction of the Mg_3Mm alloys were determined by using the van't Hoff equation as follows:

$$\ln P = \frac{\Delta H}{RT} - \frac{\Delta S}{R} \tag{1}$$

where P is plateau pressure (in absolute atmospheres), T is temperature (in K), R is gas constant (0.0083145 kJ/K mol). The obtained ΔH and ΔS for dehydriding reaction are −74.5 kJ/mol H_2 and −0.128 kJ/K mol H_2, respectively. The PCIs curves used for van't Hoff plot were measured after the sample had gone two hydrogenation/dehydrogenation cycles at 300 °C.

Fig. 5 gives van't Hoff plots of Mg_3Mm. For comparison, van't Hoff plots of Mg and Mg_2Ni were also given by using the data given in Ref. [18]. Judging from Fig. 5, the most stable hydride systems is Mg_3Mm–H among the Mg and Mg_2Ni and Mg_3Mm alloys systems,

Hydrogen absorption kinetic curve of the Mg_3Mm alloy was measured at room temperature as the alloy can absorb hydrogen at this temperature. Typical hydriding kinetic curve of Mg_3Mm alloy is shown in Fig. 6. It shows that the uptaking time for hydrogen content reaching 90% of the maximum storage capacity for Mg_3Mm alloy is less than 10 min. It was also found that the experimental kinetic curve for Mg_3Mm alloy fitted best to Avrami–Erofeev equation (Eq. (2)) based on nucleation and growth process:

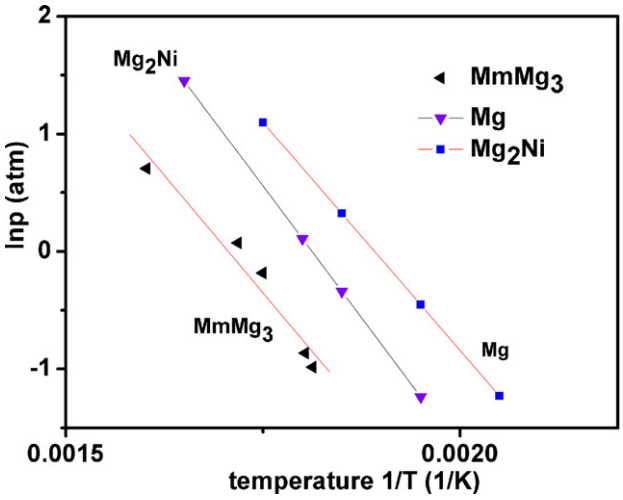

Fig. 5. van't Hoff plot of different hydrogen storage alloys. The plot for Mg_3Mm was made after the data measured in this work. The plot for Mg and Mg_2Ni was made after the data given in Ref. [18].

$$\alpha(t) = 1 - \exp(-Bt^m) \tag{2}$$

where $\alpha(t)$ is the reaction rate, meaning the ratio of the reacted material to the total material, B and m are constants, and t is reaction time.

The values of B and m obtained by fitting are shown in Fig. 6. The error was estimated by factor S (the standard error) and r (the correlation coefficient), which are also given in Fig. 6. It can be seen from the values of S and r that the fitting is in excellent agreement with the experiment data. This result confirms that the hydriding reaction of the Mg_3Mm alloy obeys the nucleation and growth mechanism, which is similar to other metal hydride [7]. However, different m values indicate different rate controlling step of nucleation and growth reaction. With respect to the alloy investigated in this work, m value is close to 0.62, which suggests that the hydriding of Mg_3Mm alloy at room temperature is basically a one-dimensional diffusion-controlled nucleation and growth process.

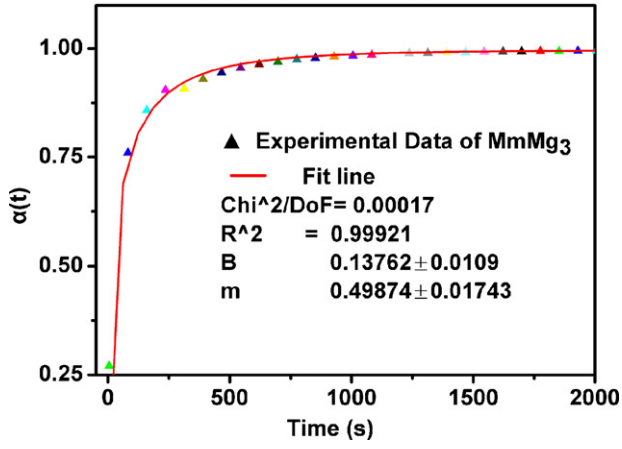

Fig. 6. Hydriding kinetic curves of Mg_3Mm alloy measured under a hydrogen pressure of 3.5 MPa at room temperature and their fitting curves.

4. Summary

The present work demonstrates that Mg_3RE intermetallic compounds have promising hydrogen storage properties. The addition of Ni lowers the dehydrogenation temperature but also decreases the hydrogen storage content. XRD analysis proved that phase structure changed during hydrogenation/dehydrogenation. The $D0_3$ type structured Mg_3RE with lattice constant being 0.7451 nm transformed to an unknown fcc structure with lattice constant being 0.5606 nm after hydrogenation. PCIs measurement shows that the maximum hydrogen absorption contents of Mg_3Mm and $Mg_3MmNi_{0.1}$ alloy are 2.91 and 2.51 wt.%, respectively. Mg_3Mm and $Mg_3MmNi_{0.1}$ alloys could absorb hydrogen at room temperature and desorb hydrogen at 281 and 251 °C, respectively. Mg_3Mm alloy exhibits rapid hydriding and dehydriding kinetics. The hydriding reaction obeys a rate equation governed by a one-dimensional diffusion-controlled nucleation and growth process. The refueling time is less than 10 min for them to uptake 90% of its full hydrogen absorption content.

Acknowledgements

This work was supported by NSFC under project Nos. 50401015 and 50631020, PCSIRT (No. IRT0551), NCET and Guangdong Provincial Natural Science Foundation (Team project).

References

[1] A. Zaluska, L. Zaluski, J.O. Ström-Olsen, Appl. Phys. A 72 (2001) 157–165.
[2] K. Yvon, B. Bertheville, J. Alloys Compd. 425 (2006) 101–108.
[3] M. Tsuda, W.A. Diño, H. Kasai, H. Nakanishi, H. Aikawa, Thin Solid Films 509 (2006) 157–159.
[4] G. Barkhordarian, T. Klassen, R. Bormann, Scripta Mater. 49 (2003) 213–217.
[5] K.S. Jung, E.Y. Lee, K.S. Lee, J. Alloys Compd. 421 (2006) 179–184.
[6] A. Bakkar, V. Neubert, Corros. Sci. 47 (2005) 1211–1225.
[7] L.Z. Ouyang, H. Wang, C.Y. Chung, J.H. Ahn, M. Zhu, J. Alloys Compd. 422 (2006) 58–61.
[8] W.P. Kalisvaart, R.A.H. Niessen, P.H.L. Notten, J. Alloys Compd. 417 (2006) 280–291.
[9] P. Vermeulen, R.A.H. Niessen, P.H.L. Notten, Electrochem. Commun. 8 (2006) 27–32.
[10] P. Selvam, B. Viswanathan, C. Swamy, V. Srinivasan, Int. J. Hydrogen energy 11 (1986) 169–192.
[11] S. Yajima, H. Kayano, H. Toma, J. Less-Common Met. 55 (1977) 139–141.
[12] K.H.J. Buschow, J. Less-Common Met. 44 (1976) 301–306.
[13] V.V. Karonik, D.N. Kazakov, R.A. Andrievskii, O.P. Bogachkova, Org. Mater. 20 (1984) 207–211.
[14] A. Kamegawa, Y. Goto, H. Kakuta, H. Takamura, M. Okada, J. Alloys Compd. 408 (2006) 284–287.
[15] Q.A. Zhang, Y.J. Liu, T.Z. Si, J. Alloys Compd. 417 (2006) 100–103.
[16] L.Z. Ouyang, F.X. Qin, M. Zhu, Scripta Mater. 55 (2006) 1075–1078.
[17] G. Renaudin, L. Guénée, K. Yvon, J. Alloys Compd. 350 (2003) 145–150.
[18] D. Taizhang, The properties and application of metal-hydride, Japan, 1999, ISBN4-900041-72-6.